

Reference-phantom-free imaging of local attenuation coefficient in synthetic transmit aperture ultrasound imaging

Khalid Abdalla, Na Zhao, and Yuan Xu^{a)}

Physics Department, Toronto Metropolitan University, Toronto, ON, M5B 2K3, CA

k1abdalla@torontomu.ca, na.zhao@torontomu.ca, yxu@torontomu.ca

Abstract: The attenuation coefficient slope (ACS) is an essential property of biological tissues. Most of the present ACS estimation methods use spectrum-based approaches in B-mode imaging and need a reference phantom. A method to map ACS without a reference phantom is proposed in Synthetic Transmit Aperture ultrasound imaging. The diffraction effect in ACS estimation is studied. In this paper, the transducer bandwidth was divided into overlapping sub-bands, and each sub-band was used to reconstruct an image and yield the corresponding sub-band attenuation coefficient to obtain ACS. The feasibility of the proposed method was demonstrated in numerical simulations and experiments.

[Editor: —]

<https://doi.org/>

Date: 12 November 2024

1. Introduction

Ultrasound imaging plays a vital role in medical diagnostics, providing real-time visualization of anatomical structures and assisting in detecting and characterizing various diseases. The attenuation coefficient is a fundamental parameter in ultrasound imaging^{1,2}. Usually, The attenuation coefficient is proportional to frequency in biological tissues. Therefore, the attenuation coefficient slope (ACS), the ratio between the attenuation coefficient and frequency, is used to describe attenuation in tissues. Two different attenuation parameters have been considered in the literature. First, there is the local attenuation. The local attenuation is the attenuation within a region of interest and is used primarily to quantify the tissue properties of that region. The second one is the total attenuation. The total attenuation is the effective attenuation along the propagation path from the source through the intervening tissue layers to the region of interest³. Local attenuation is studied in this paper.

ACS provides valuable information about tissue composition and can be instrumental in assessing liver diseases, like fibrosis and steatosis, imaging breasts, and monitoring therapy response^{1,2}. It also plays a role in other Quantitative Ultrasound (QUS) methods, like particle size estimation. Several power-spectrum-based techniques have been developed to estimate the ultrasound attenuation coefficient. For instance, the spectral-shift method estimates ACS by measuring the downshift in the center frequency of the radio-frequency signals with depth. This method assumes that the radiofrequency (RF) envelope's spectral shape resembles a Gaussian curve³. Conversely, reference phantom methods, which include the spectra difference method, spectra log difference method, and the hybrid method, use phantoms with known ACS and scattering properties to account for the diffraction effect and other system effects, including the transducer response function. The diffraction effect [factor $D(f_i, z)$ in Eq. 1], is the effect of the ultrasound beam converging and diverging on the attenuation estimation in B-mode imaging. For example, in the pre-focus zone of B-mode imaging, the ultrasound beam intensity increases when moving toward the focus point. This will make the estimated attenuation coefficient less than the truth value. Since the diffraction effect depends on both the frequency and depth, it can significantly impact the quality and interpretability of ultrasound attenuation estimation^{4,5}. Recent studies have explored regularization techniques with a spatial prior^{5,6} and a tomography approach where local ACS distribution in ROI was estimated simultaneously by solving a linear equation set. These approaches have shown promise in enhancing both the precision and resolution of quantitative ultrasound (QUS). However, the clinical implementation of the reference-phantom method has been slow, hindered by the need to scan a well-calibrated reference phantom with the same clinical equipment and settings used to acquire data from the patient¹.

Recently, Gong et al.⁷ introduced a reference-phantom-free method, the reference frequency method. It used planar wave imaging to acquire the data. It normalized the system effects by calculating the ratio between the power spectra of each frequency and its adjacent frequency to estimate ACS without a well-calibrated phantom. Rafati⁸ applied the reference frequency method with parametric regularization to reduce the window size to about 1 cm and to alleviate image artifacts. However, it is still unclear if the diffraction effect can be addressed successfully by the normalization process for array configurations other than the one used in these papers, such as different central frequencies and elevational focus distances. In the reference frequency method⁷, the logarithm of the ratio between the power spectra of each frequency and its adjacent frequency is mathematically equivalent to taking the frequency derivative of the logarithm of the power spectra, which generally will not cancel out the diffraction term completely (see Eq. 3). The diffraction effect has been compensated successfully in attenuation imaging when a single spherically focused transducer was used by including a diffraction factor in attenuation estimation^{3,2}. However, In most clinical ultrasound imaging, a one-dimensional linear or phased array is used because B-mode images with a single element are optimally focused only around the focus point. The spatial resolution of the B-mode image will be compromised in the off-focus region. In a 1D array probe, the lateral focusing is provided by controlling the timing of array elements and the elevational focusing is achieved by an acoustic lens with a fixed focus. No study on the diffraction factor for one-dimensional linear or phased arrays has been reported in attenuation estimation.

In traditional B-mode imaging methods, multiple elements are activated in a timed sequence to emit a focused wave in each transmission. ACS is often estimated based on the power spectrum, calculated from segments of each A-line,

^{a)} Author to whom correspondence should be addressed.

and noise in the power spectrum is typically reduced by averaging over many adjacent A-lines. However, the high speckle variation in B-mode images still results in significant noise in the ACS estimation, necessitating either larger estimation window or regularization methods to improve accuracy.

To overcome the above challenges, we propose a method of imaging ACS without using a reference phantom in the Synthetic Transmit Aperture (STA) ultrasound imaging. In STA, a transducer element transmits an unfocused spherical wave covering the entire image, one element at a time, while all or a part of the aperture elements sample the backscattered signals. If the nonlinear effect is ignored, the STA data set has more information than B-mode because B-mode data can be synthesized from STA data, while the process to recover STA data from B-mode is subject to introducing noise in principle and needs regularization⁹. We propose to apply a recently developed method, the decorrelated compounding (DC) method, to suppress speckle noise to increase the accuracy of estimating the attenuation coefficient¹⁰.

To study the feasibility of an imaging ACS without using a reference phantom, we investigate the diffraction effect in STA. Unlike B-mode imaging, which focuses at one point, the Synthetic Transmit Aperture (STA) image can be optimally focused at every image point along the lateral direction, which minimizes the diffraction effect in ACS estimation caused by the laterally focusing. However, the elevational focusing is achieved by an acoustic lens with a fixed focus. Therefore, the ultrasound beam profile will still change with depth due to the elevational focus. Therefore it is unclear if the diffraction effect is significant in the proposed method. We will investigate how the diffraction effect will affect the ACS estimation in STA imaging.

The structure of this paper is as follows: Section 2 introduces the modelling of backscattered ultrasound signals, presents the theoretical foundation for ACS estimation, and describes the simulation and experiment studies. The experimental setups, including simulations and tissue-mimicking phantoms, are also explained. In Section 3, the results from both the simulation and phantom studies are presented. Section 4 discusses the strengths and limitations of ACS estimation in synthetic aperture imaging and potential future research directions. Finally, Section 5 concludes the paper.

2. Method

2.1 Theory

In most local attenuation estimation studies^{4,11}, the power spectrum of the RF signals from a region of interest (ROI) centred at depth z_0 is estimated first, then ACS is estimated from the power spectrum. In this paper, we reconstruct the ROI image from the i -th sub-band RF signals with central frequency, f_i . The attenuation coefficient μ at f_i is estimated directly by taking the depth derivative of the sub-band ROI image due to reduced image noise through using decorrelated compounding. Lastly, ACS is obtained by taking the linear fitting of the attenuation coefficients over the frequencies, which is equivalent to taking the frequency derivative.

The power spectrum of the received RF signals from a scattering medium at the i -th sub-band can be approximately modelled by the following equation.^{4,11}

$$S(f_i, z) = C^2(f_i) \cdot D(f_i, z) \cdot BSC(f_i, z) \cdot A(f_i, z), \quad (1)$$

where $C(f_i) = G \cdot V(f_i) \cdot U^2(f_i)$ is the transducer related factor including the electrical signal $V(f_i)$ driving the transducer, the transducer response function $U(f_i)$, and an electromechanical coupling constant G ; $D(f_i, z)$ is the diffraction effect, $BSC(f_i, z)$ is the pressure backscatter coefficient within the ROI, $A(f_i, z) = e^{-4 \int_0^z \mu(f_i, z') / 8.69 dz'}$ represents the attenuation along the propagation path from the transducer to the point at depth z , $\mu(f_i, z')$ (in dB/cm-MHz) is the frequency-dependent attenuation coefficient at z' , and the factor 8.69 is used to convert dB to Np. For biological tissues, it is usually assumed $\mu(f_i, z') = \alpha(z') f_i$ for simplicity, where $\alpha(z')$ is the attenuation coefficient slope at z' in dB/(cm - MHz).

In this paper, we assume $BSC(f_i, z)$ doesn't change with depth within a homogeneous region of interest (ROI) used to estimate attenuation. The limitation of this assumption will be addressed in the discussion section. Taking the natural logarithm of equation (1), the attenuation coefficient (μ) can be expressed as the derivative of pressure amplitude over the depth (z) direction in ROI,

$$\mu(f_i, z) = -\frac{1}{4} \left(\frac{\partial \ln(S(f_i, z))}{\partial z} - \frac{\partial \ln(D(f_i, z))}{\partial z} \right). \quad (2)$$

To reduce the noise in the estimated μ , we use the linear fitting of the image value in an ROI over the depth to find the μ for an ROI. Considering the linear frequency dependence of attenuation coefficient in biological tissues, we have

$$\alpha(z) = -\frac{1}{4} \left(\frac{\partial^2 \ln(S(f_i, z))}{\partial z \partial f} - \frac{\partial^2 \ln(D(f_i, z))}{\partial z \partial f} \right). \quad (3)$$

In the reference frequency method⁷, the ACS is found by taking the depth-derivative of the logarithm of the ratio between the power spectra of each frequency and its adjacent frequency. This process is mathematically equivalent to changing the $\partial z \partial f$ in Eq. 3 into $\partial f \partial z$. Therefore, the reference frequency method⁷ is mathematically equivalent to our method. Nevertheless, the novelty of the proposed method is to use decorrelated compounding to reduce the speckle noise and to investigate if the diffraction effect is significant in the proposed method.

2.2 Decorrelated compounding in STA

To reduce the speckle variation in the ultrasound image, the method of Decorrelated Compounding in Synthetic Transmit Aperture (DC in STA)¹⁰ was adapted to obtain the pressure amplitude of the backscattered signals $P(f_i, z)$. The reduced speckle variation can improve the accuracy of attenuation coefficient estimation. In DC, the aperture domain of the RF data was divided into sub-apertures using a translating and overlapping window in the aperture domain. The Delay-and-Sum image reconstruction algorithm was applied to these sub-aperture signals, reconstructing a series of sub-aperture images. The eigenvectors and eigenvalues of the covariance matrix for the sub-aperture images were used to remove the correlation among the sub-aperture images before incoherent compounding in¹⁰. Theoretically, the averaged variance of N uncorrelated sub-images can be reduced by a factor of \sqrt{N} . Therefore, the decorrelation procedure can improve the speckle variance reduction performance by removing the correlations among sub-aperture images over the traditional incoherent compounding¹⁰.

In this paper, we only applied decorrelated compounding to the sub-images within the same temporal sub-band spectrum to obtain the attenuation coefficient corresponding to the sub-band frequency. The compounding result for each sub-band is denoted as the pressure amplitude $P(f_i, z)$ for the selected sub-band f_i . We used a sub-aperture of 16 elements to reconstruct one sub-image. The step size between the two adjacent sub-apertures was 8 elements. These configurations were the same in the transmission and receiving apertures, resulting in 16 sub-apertures along the transmission and receiving dimensions. The total number of sub-apertures/sub-images for one sub-band was $N_{SC} = 25$. Therefore, the speckle SNR is expected to improve by 5 times. The bandwidth of a sub-band and the step size for the adjacent two sub-bands were 0.6 MHz and 0.3 MHz, respectively.

2.3 Simulation and experiment configurations

To investigate how the diffraction effect will affect the ACS estimation in STA imaging, we imaged two simulation phantoms: one with attenuation, ACS $\alpha = 0.7$ dB/cm-MHz, and one without attenuation, ACS $\alpha = 0.0$ dB/cm-MHz. A scattering medium with an ACS $\alpha = 0.0$ dB/cm-MHz, is used to represent the contribution from the diffraction effect, the second term in Eq. 3. After finding the ACS profiles for both phantoms, we subtract them to obtain the corrected ACS.

To effectively estimate the attenuation, an ROI window of size 1 cm x 2 cm, centered at depth z_0 , is employed. Within this window, there are 50 vertical image lines, each spaced 0.20 mm apart laterally. To enhance the signal-to-noise ratio of the estimated ACS, results from the central 30 image lines within this window were averaged. The adjacent ROIs have a substantial overlap of 98% along the depth direction.

To implement the derivative over the depth and frequency, linear regression was applied to the ROI to obtain μ first, and then α , the attenuation coefficient slope. In order to mitigate potential errors arising from the noise in RF signals, the fitting for the attenuation coefficient slope was restricted to a frequency range of 6.3-9.5 MHz in simulations, around the central frequency of the probe¹².

The proposed method was tested using the simulated and experimental RF data. For the simulation model, The Field II Simulation package was employed to generate RF data from speckle-generating phantoms¹³. A 128-element phased array transducer has a width of 2.79 cm, a nominal frequency of 7.8 MHz, and no elevational focus (or equivalently focused at infinite far away). The probe was positioned 1 cm above the phantoms. The sound wave velocity of 1540 m/s was adopted. A complete set of synthetic aperture data was sampled at a rate of 24 MHz. The dimensions of the reconstructed image were 8 cm in the axial direction and 2.79 cm in the lateral direction for each sub-band image.

The Verasonics Vantage Research Platform (Verasonics Inc., Kirkland, WA) with a P6-3 probe was used to acquire the experimental RF data from a model 040GSE (CIRS Inc., Norfolk, VA) phantom. A 128-element phased array transducer has a width of 2.79 cm, a nominal frequency of 4.4 MHz, and the elevational focus is unknown. The attenuation in the imaged areas was $\alpha = 0.7$ dB/cm-MHz and the acoustic wave velocity was 1540 m/s according to the specifications provided by the manufacturer.

The simulation and experiment STA data were processed using the delay-and-sum beamforming to reconstruct the sub-images from the sub-band and sub-aperture RF signals. Then, the decorrelated compounding method was used to reduce the speckles in the sub-images before the attenuation coefficient estimation procedure in section 2.1.

3. Results

3.1 Effectiveness of the decorrelated compounding method

Linear regression analysis of image intensity values at various depth points was performed to estimate the attenuation slopes (dB/cm) for each sub-band. At shallow depths (4 cm), the attenuation coefficients followed a linear trend (black line in Fig.1) across the frequency range, including higher frequency components 9.5 MHz, as expected from the linear dependence of attenuation coefficient on frequency. However, at deeper depths (6.9 cm), the higher frequency components deviated from the linear trend as shown by the blue line in Fig.1. Therefore, we chose only the range of frequency where the linear dependence stands, as shown by the green line in Fig.1.

3.2 Simulation results of ACS mapping

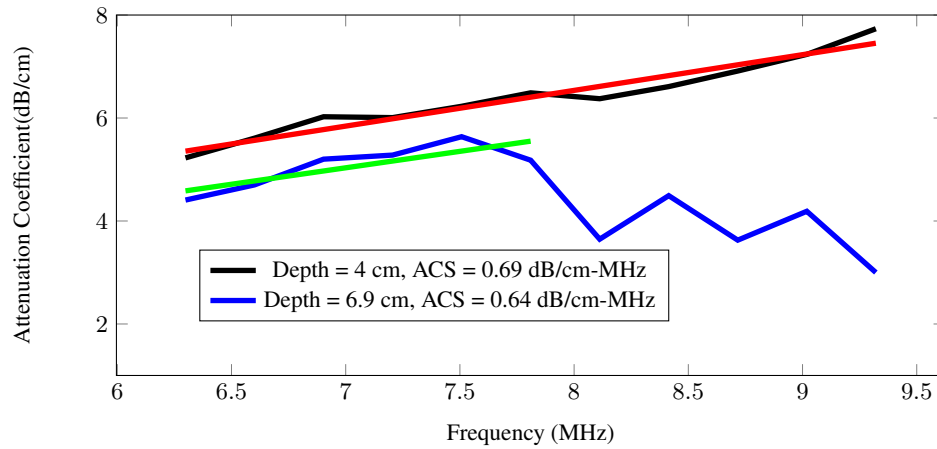


Fig. 1. Linear Relationship of dB/cm vs. Sub-Band frequencies at 4 cm depth (black) and 6.9 cm (blue) within the selected frequency range in a 0.7 dB/cm-MHz phantom

The ACS values of simulated phantoms are plotted as a function of depth in Fig. 2. The simulations include: Phantom 1 (blue), with an ACS $\alpha = 0.7$ dB/cm-MHz, and non-attenuating phantom (dashed blue), with an ACS $\alpha = 0.0$ dB/cm-MHz. The non-attenuating phantom was used to account for the diffraction effect. The corrected ACS values (green) were obtained by subtracting the baseline phantom ACS values from Phantom 1 (blue). The corrected ACS values were obtained by subtracting non-attenuating phantom results from the attenuating phantom, and it is closely aligned with the expected value of 0.7 dB/cm-MHz. Specifically, ACS values between 2 cm and 3 cm were improved, indicating that baseline subtraction effectively accounts for system-related artifacts and diffraction effects. For the corrected ACS values (covering a depth range from 2 cm to 7 cm), the mean attenuation is 0.68 ± 0.03 dB/cm-MHz, close to the true value. However, the corrected ACS values still display underestimation at deeper depths (beyond 6.9 cm). We will discuss this failure in the discussion section.

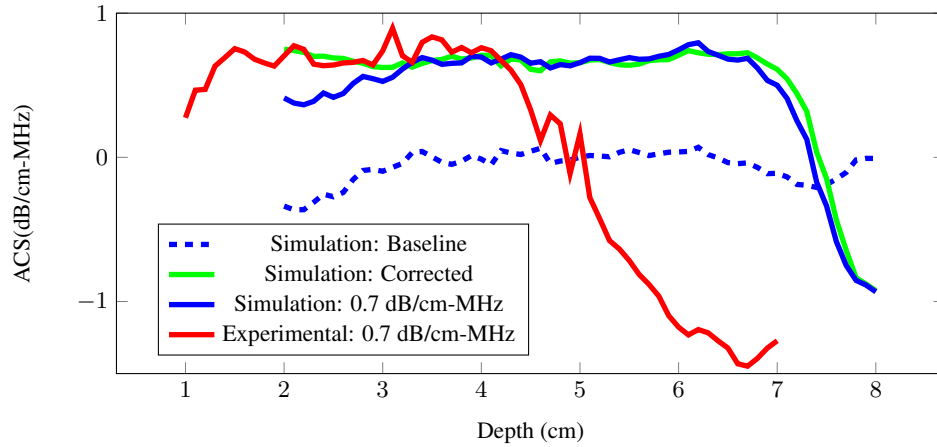


Fig. 2. ACS values vs. depth for simulated and experimental Phantoms. **The simulation results** include Phantom 1 (blue) with an ACS of 0.7 dB/cm-MHz, exhibiting expected attenuation but with underestimation beyond 6.9 cm. The baseline phantom (dashed blue) represents a zero-attenuation (0.0 dB/cm-MHz) condition, accounting for system noise and diffraction effects. The corrected ACS values (green) were obtained by subtracting baseline values from Phantom 1, aligning closely with 0.7 dB/cm-MHz between 2 cm and 3 cm, indicating effective diffraction correction but still showing underestimation beyond 6.9 cm. **Experimental results** for the CIRS phantom (red) with a true ACS of 0.7 dB/cm-MHz display underestimation from 1 cm to 1.5 cm, accurate ACS between 1.6 cm and 4.5 cm, and a sharp decrease beyond 4.5 cm.

3.3 Tissue-mimicking experimental phantoms

To evaluate the ACS estimation performances quantitatively in tissue-mimicking experimental phantoms, we selected a uniform region of CIRS phantoms. Fig. 2 illustrates the plot of the estimated ACS versus depth for CIRS phantom (red) of 0.7 dB/cm-MHz. The ACS was estimated as close to the probe as 1.0 cm, which was not reported in other methods. From 1 cm to 1.5 cm, the ACS values were underestimated, likely due to near-field diffraction and system effects. Between 1.6 cm and 4.5 cm, the mean ACS was approximately 0.7 ± 0.08 dB/cm-MHz, closely aligning with the expected attenuation coefficient. Beyond 4.5 cm, the ACS values sharply decreased, indicating the failure of the method at this depth.

4. Discussion

This study presents a reference-phantom-free approach for estimating the attenuation coefficient slope in Synthetic Transmit Aperture imaging, enhanced with decorrelated compounding to minimize speckle noise. Results indicate that diffraction effects significantly impact ACS estimation at shallow depths, underscoring the importance of managing these effects.

In Fig. 1, the linear dependence of attenuation on frequency for the signals at 6.9 cm was maintained only up to the transducer's nominal frequency of 7.8 MHz in simulations. An initial analysis into the decorrelated sub-band images suggested that the deviation from linear relationship might be due to the decorrelated compounding process. We found that at high frequency, the decorrelated sub-band image values dropped quickly. ACS values showed underestimation at deeper depths (beyond 6.9 cm in simulations and beyond 4.5 cm in experiments in Fig. 2), likely due to the same reason. We plan to investigate some parameter adjustments in the decorrelated compounding at high frequency range in the future. The parameters that can be optimized to improve the spatial resolution and estimation accuracy include sub-aperture configuration, the number of decorrelated sub-images for incoherent compounding, and ROI size. At greater depths, estimated ACS results showed some bias and fluctuation, suggesting that constrained optimization and regularization methods, as used in other ACS estimation approaches^{8,9,14} could enhance accuracy. Though not applied in this study, future work could incorporate these techniques to reduce bias and improve precision.

To enhance ACS estimation accuracy, future work will focus on calculating and applying the diffraction factor from theory. This will involve deriving a simplified approximation of the two-fold integration^{15,16} to calculate the diffraction factor for a one-dimensional linear or phased array¹⁷. We will consider the focus along both the lateral and elevation direction, follow the strategy in^{15,16}, and use the field profile of a rectangular aperture in¹⁸. The derived simplified diffraction factor will be validated against the Field II simulations and experimental phantom for quantitative ultrasound imaging. The diffraction factor of a probe can also be estimated by imaging a homogeneous random medium with a particle size much smaller than the ultrasound wavelength.

The approach, though developed for STA, also has potential for adaptation to B-mode. Recovering STA data from pre-beamformed B-mode data through regularization^{9,14,19} may enable broader application, although the effects of information loss in this process need evaluation.

5. Conclusion

In conclusion, we proposed using the decorrelated compounding (DC) method to estimate the attenuation coefficient slope (ACS) within Synthetic Transmit Aperture (STA) ultrasound imaging. Attenuation measurements from simulations and tissue-mimicking phantoms demonstrate the effectiveness of this approach for ACS estimation. Compared to traditional B-mode imaging, STA offers enhanced accuracy in quantifying tissue properties by reducing diffraction effects and improving signal consistency. Further research and comparative studies will be essential to validate these findings and to fully explore the clinical potential of STA in providing precise, reference-phantom-free ACS estimation.

Acknowledgment

The authors would like to thank the following funding agencies: Natural Sciences and Engineering Research Council of Canada (NSERC), Canada Foundation for Innovation (CFI), and Toronto Metropolitan University.

References and links

- ¹ M. L. Oelze and J. Mamou, "Review of quantitative ultrasound: Envelope statistics and backscatter coefficient imaging and contributions to diagnostic ultrasound," *IEEE Transactions on Ultrasonics, Ferroelectrics, and Frequency Control* **63**, 336–351 (2016) doi: [10.1109/TUFFC.2015.2513958](https://doi.org/10.1109/TUFFC.2015.2513958).
- ² G. Cloutier, F. Destrempes, F. Yu, and A. Tang, "Quantitative ultrasound imaging of soft biological tissues: a primer for radiologists and medical physicists," *Insights into Imaging* **12**, 1–20 (2021).
- ³ T. A. Bigelow and Y. Labyed, "Attenuation compensation and attenuation," in *Quantitative Ultrasound in Soft Tissues* (Springer Dordrecht, 2013).
- ⁴ L. X. Yao, J. A. Zagzebski, and E. L. Madsen, "Backscatter coefficient measurements using a reference phantom to extract depth-dependent instrumentation factors," *Ultrasonic imaging* **12**(1), 58–70 (1990).
- ⁵ A. L. Coila and R. Lavarello, "Regularized spectral log difference technique for ultrasonic attenuation imaging," *IEEE transactions on ultrasonics, ferroelectrics, and frequency control* **65**(3), 378–389 (2017).

- ⁶ Z. Vajihi, I. M. Rosado-Mendez, T. J. Hall, and H. Rivaz, "Low variance estimation of backscatter quantitative ultrasound parameters using dynamic programming," *IEEE transactions on ultrasonics, ferroelectrics, and frequency control* **65**(11), 2042–2053 (2018).
- ⁷ P. Gong, P. Song, C. Huang, J. Trzasko, and S. Chen, "System-independent ultrasound attenuation coefficient estimation using spectra normalization," *IEEE transactions on ultrasonics, ferroelectrics, and frequency control* **66**(5), 867–875 (2019).
- ⁸ I. Rafati, F. Destrepes, L. Yazdani, M. Gesnik, A. Tang, and G. Cloutier, "Regularized ultrasound phantom-free local attenuation coefficient slope (acs) imaging in homogeneous and heterogeneous tissues," *IEEE Transactions on Ultrasonics, Ferroelectrics, and Frequency Control* **69**(12), 3338–3352 (2022).
- ⁹ P. Gong, M. C. Kolios, and Y. Xu, "Delay-encoded transmission and image reconstruction method in synthetic transmit aperture imaging," *IEEE Transactions on Ultrasonics, Ferroelectrics, and Frequency Control* **62**(10), 1745–1756 (2015) doi: [10.1109/TUFFC.2015.007005](https://doi.org/10.1109/TUFFC.2015.007005).
- ¹⁰ N. Zhao and Y. Xu, "Decorrelated compounding improves lesion signal-to-noise ratio of low-contrast lesions in synthetic transmit aperture ultrasound imaging," *JASA Express Letters* **2**(2), 022001 1–8 (2022) doi: [10.1121/10.0009385](https://doi.org/10.1121/10.0009385).
- ¹¹ K. Nam, J. A. Zagzebski, and T. J. Hall, "Simultaneous backscatter and attenuation estimation using a least squares method with constraints," *Ultrasound in medicine & biology* **37**(12), 2096–2104 (2011).
- ¹² K. Nam, I. M. Rosado-Mendez, N. C. Rubert, E. L. Madsen, J. A. Zagzebski, and T. J. Hall, "Ultrasound attenuation measurements using a reference phantom with sound speed mismatch," *Ultrasonic imaging* **33**(4), 251–263 (2011).
- ¹³ J. A. Jensen, "Field: A program for simulating ultrasound systems," *Medical & Biological Engineering & Computing* **34**(sup. 1), 351–353 (1997).
- ¹⁴ N. Bottenus, "Recovery of the complete data set from focused transmit beams," *IEEE Transactions on Ultrasonics, Ferroelectrics, and Frequency Control* **65**, 30–38 (2018) doi: [10.1109/TUFFC.2017.2773495](https://doi.org/10.1109/TUFFC.2017.2773495).
- ¹⁵ M. F. Insana, R. F. Wagner, D. G. Brown, and by Ishimaru, "Describing small-scale structure in random media using pulse-echo ultrasound," *J. Acoust. Soc. Am* **87** (1990) <http://acousticalsociety.org/content/terms>.
- ¹⁶ N. X. Chen, D. Phillips, K. Schwarz, J. Mottley, and K. Parker, "The measurement of backscatter coefficient from a broadband pulse-echo system: a new formulation," *IEEE Transactions on Ultrasonics Ferroelectrics and Frequency Control* **44**(2), 515–525 (1997) <https://doi.org/10.1109/58.585136> doi: [10.1109/58.585136](https://doi.org/10.1109/58.585136).
- ¹⁷ N. Zhao, S. Sharma, and Y. Xu, "Estimating autocorrelation function of a scattering medium in synthetic transmit aperture ultrasound imaging," **In preparation** (DOI 10.32920/24471244, 2024).
- ¹⁸ T. D. Mast, "Fresnel approximations for acoustic fields of rectangularly symmetric sources," *The Journal of the Acoustical Society of America* **121**(6), 3311–3322 (2007) <https://doi.org/10.1121/1.2726252> doi: [10.1121/1.2726252](https://doi.org/10.1121/1.2726252).
- ¹⁹ D. Hyun, J. J. Dahl, and N. Bottenus, "Real-time universal synthetic transmit aperture beamforming with retrospective encoding for conventional ultrasound sequences (refocus)," in *2021 IEEE International Ultrasonics Symposium (IUS)* (2021), pp. 1–4, doi: [10.1109/IUS52206.2021.9593648](https://doi.org/10.1109/IUS52206.2021.9593648).